



# Optical clearing agent increases effectiveness of photodynamic therapy in a mouse model of cutaneous melanoma: an analysis by Raman microspectroscopy

LETÍCIA PALOMBO MARTINELLI,<sup>1,2,4</sup>  IEVGENIIA IERMAK,<sup>2</sup> LILIAN TAN MORIYAMA,<sup>2</sup> MICHELLE BARRETO REQUENA,<sup>2</sup> LAYLA PIRES,<sup>3</sup> AND CRISTINA KURACHI<sup>1,2,5</sup> 

<sup>1</sup>Federal University of São Carlos, Post-Graduation Program in Biotechnology, Rodovia Washington Luís km 235, SP-310, São Carlos 13565-905, Brazil

<sup>2</sup>University of São Paulo, São Carlos Institute of Physics, Avenue Trabalhador São-Carlense, 400, São Carlos, São Paulo 13566-590, Brazil

<sup>3</sup>Princess Margaret Cancer Center, University Health Network, Princess Margaret Cancer Research Tower, 101 College Street, Toronto, Ontario M5G1L7, Canada

<sup>4</sup>leticia.martinelli@usp.br

<sup>5</sup>cristina@ifsc.usp.br

**Abstract:** Melanoma is the most aggressive type of skin cancer and a relevant health problem due to its poor treatment response with high morbidity and mortality rates. This study, aimed to investigate the tissue changes of an improved photodynamic therapy (PDT) response when combined with optical clearing agent (OCA) in the treatment of cutaneous melanoma in mice. Photodithazine (PDZ) was administered intraperitoneally and a solution of OCA was topically applied before PDT irradiation. Due to a resultant refractive index matching, OCA-treated tumors are more optically homogenous, improving the PDT response. Raman analysis revealed, when combined with OCA, the PDT response was more homogenous down to 725  $\mu\text{m}$ -depth in thickness.

© 2020 Optical Society of America under the terms of the [OSA Open Access Publishing Agreement](#)

## 1. Introduction

Melanoma is a pigmented tumor that originates from the melanocytes. According to the National Cancer Database (NCDB-US) the most prevalent type of melanoma is the cutaneous form (91.2%), followed by ocular, mucosal and other tissues [1]. Cutaneous melanoma is the most aggressive type of skin cancer. It is characterized by pigmented lesions with a high rate of tissue invasion and metastasis [2]. It accounts for about 80% to 85% of all skin cancer-related deaths [3].

The main therapy approach for cutaneous melanoma is surgery, with wide excision of the cutaneous lesion, lymphatic mapping, sentinel lymph node biopsy and lymph node dissection [4,5]. The width of the surgical excision of melanoma is related to the Breslow index, a thickness tumor measurement, indicating the depth of the melanoma from the skin surface down through to its deepest point. The present recommendations for definitive wide local excision of primary cutaneous melanoma are melanoma in situ: 5-10 mm margins, invasive melanoma (pT1)  $\leq 1.0$  mm thick: 1 cm margins, invasive melanoma (pT2) 1.01-2.00 mm thick: 1-2 cm margins, invasive melanoma (pT3) 2.01-4.00 mm thick: 1-2 cm margins and invasive melanoma (pT4)  $> 4.0$  mm thick: 2 cm margins [6-8]. A typical Breslow index (thickness) of melanomas, when diagnosed by dermatologists, varies slightly, with the majority being diagnosed with  $< 1$  mm of thickness and with a high chance of cure (70%), but there are cases where melanoma is diagnosed with a thickness  $> 1$  mm with poor survival rates [9]. Adjuvant immunotherapy,

palliative chemotherapy, and radiotherapy are also used, but they have limited effect on patients' life expectancy [10–12]. Because of the lack of effective therapeutic options and the increased incidence of melanoma, the development of new non-invasive diagnostic techniques, as well as of novel treatments is required.

Photodynamic therapy (PDT) is based on the interaction between light and photosensitizer (PS), in the presence of molecular oxygen, to induce cell death. PDT has been widely used for localized treatment of several types of cancer, such as cervical [13], esophageal [14], stomach [15,16], bladder [15,17], and nonmelanoma skin [18–20]. PDT clinical trials in basal cell carcinoma (BCC) show a complete response rate around 85% [18–21]. More recently, this success rate has been approaching 93% in a single visit PDT protocol for superficial and nodular BCC lesions [22]. For cutaneous melanoma, the few reported clinical trials have shown that PDT reduces the volume of the lesion but does not eliminate it, due to its significant resistance [23–27].

The main limitation of PDT for melanoma treatment is related to the high light absorption of melanin (the pigment produced by melanosomes) at the visible range of the electromagnetic spectrum. Melanin accumulates within cells in different sized granules, which implies not only in light absorption but also results in high light scattering. These characteristics limit the propagation of light in depth, restricting any optical technique to the most superficial layers of the tumor [23,28]. Additionally, melanin presents an antioxidative effect [29], and the melanoma cells show an effective mechanism for drug efflux [30–32], both characteristics that reduce the PDT response.

One approach to increase PDT response would be to change the optical characteristics of melanoma, improving light distribution within the lesion, mostly its penetration in depth. One strategy to achieve this is by using optical clearing agent (OCA). These compounds are non-toxic hyperosmotic agents such as glycerol, polyethylene glycol 400 (PEG-400), sucrose, dimethyl sulfoxide (DMSO), and others with a similar refractive index of the skin one, around 1.4 [33–35]. These agents also promote local osmotic dehydration that occurs as a result of water exiting the cell more rapidly than the OCA enter after application [34]. Consequently, water is extracted from the cells and/or collagen fibers. These processes provide an additional effect of matching the refractive index of skin with OCA due to the reduction of the water content in the interstitial space, in addition to reducing the overall thickness of the tissue and making it denser. Thus, when applied to the skin, it effectively decreases the high light scattering caused by tissue microinterfaces and increases the tissue-light penetration [33–36].

Our research group pioneered the association between OCA and PDT. In that study, full-depth eradication of pigmented melanoma was achieved when the OCA was combined with the dual-photosensitizer PDT [37]. However, the mechanisms involved in the improved response are still not completely elucidated. Previous results showed that topical application of OCA reduces the light scattering at the cutaneous melanoma model increasing the light penetration in depth which was demonstrated by diffuse reflectance spectroscopy and optical coherence tomography (OCT) [38]. In this study we aimed to investigate i) the OCA effect in the PDT immediate and mediate response, and ii) if there is any biochemical change in the tumor treated with subdose PDT, with or without OCA.

## **2. Materials and methods**

### *2.1. Cell line and animal model*

B16F10 murine melanoma cells were purchased from the American Type Cell Collection (ATCC) and were cultured in Dulbecco's Modified Eagle Medium (DMEM) with 10% fetal bovine serum and 1% penicillin-streptomycin maintained at 37 °C in an incubator with 5% CO<sub>2</sub>. For the cutaneous animal model, one million cells were intradermally injected in the flanks of 6-week old BALB/c nude mice. All animal procedures were approved by the Ethics Committee for Animal Use of the São Carlos Institute of Physics (IFSC, from the University of São Paulo,

São Carlos, SP-Brazil), document number 5500080618. The animals were examined daily for lethargy, abnormal posture, weight-loss and tumor volume, being euthanized if necessary.

## 2.2. Optical clearing agents

Our group has previously investigated [39] the optical clearing effect on skin and melanoma of several OCA mixtures such as glycerol at different concentrations and mixing solutions of PEG-400 and 1,2-propanediol at the investigated animal model. The mixture between PEG-400 and 1,2-propanediol in the ratio of 19:1, respectively, presented the best results and was chosen for use in all the present PDT experiments. They were acquired from the company Sigma-Aldrich.

## 2.3. Photodynamic therapy

The animals were anesthetized with inhaled isoflurane 5% for induction and 2% for maintenance. When the pigmented melanoma lesions achieved 1 mm in diameter, chlorin e6 (Photodithazine, VETAGRAN Company, Russia) was injected intraperitoneally at a dose of 9.0 mg/kg. The drug-light interval was 2 h 30 min, as determined in a preliminary study of Photodithazine concentration at the melanoma lesion. OCA were applied topically (approximately 300  $\mu\text{L}$ ) 15 minutes before the irradiation with a gentle massage to improve its penetration through the skin. PDT irradiation was performed using a 660 nm diode laser, delivering a total fluence of 100  $\text{J}/\text{cm}^2$  in 17 minutes.

During PDT irradiation, an aluminum foil mask was used to avoid illumination of adjacent normal tissues. Four experimental groups ( $N=3$ ) were assessed: i) control (no OCA and no PDT), ii) tumor with OCA only, iii) tumor with PDT only and iv) tumor with PDT + OCA. Using a USB2000 spectrophotometer (Ocean Optics, USA), the presence of PDZ and its relative concentration in the tumor was monitored by laser-induced fluorescence spectroscopy before and after the treatment with excitation at 532 nm (see Fig. S1). Mice cohorts were sacrificed immediately and at 7 days-post-PDT and the tumor was removed for *ex vivo* analysis. The tumors were embedded in Tissue Tek Optimal Cutting-Temperature media (Sakura Finetek, Torrance, Canada) and frozen in liquid nitrogen for cryosection. Longitudinal cuts were prepared for analysis of the skin and tumor overall profile (top to bottom).

## 2.4. Raman microspectroscopy

Raman spectra of the 60  $\mu\text{m}$ -thick cryosections were measured using a confocal Raman microscope (WITec Alpha 300 RAS, Ulm, Germany) with excitation wavelength at 785 nm and the detection range at 100–3200  $\text{cm}^{-1}$ . The approximate diameter of the laser beam at the focus point is 0.65  $\mu\text{m}$ . The spectra were collected with a 20x objective lens (Zeiss, Jena, Germany) with an

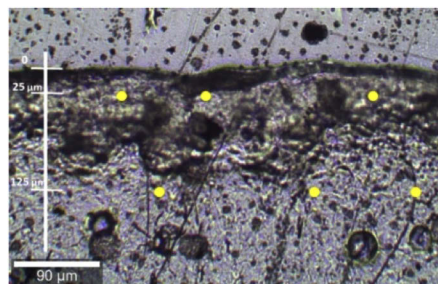


**Fig. 1.** Bright-field image of the tumor slide at the Raman confocal microscope. The spectra were reproduced in triplicate, at 3 different points at the same depth (yellow dots). The first measurement was at 25  $\mu\text{m}$ , with increments of 100  $\mu\text{m}$ , down to a 2000  $\mu\text{m}$ -depth.

integration time of 30 s and 3 accumulations for each spectrum (see Fig. S2). The duration of the Raman measurement for each sample was around 2 h, and since the tumor samples were cut through cryosectioning protocol, minimal biochemical changes are expected to occur during this analysis period. Three spectra were acquired for each depth within the tumor; measurements were taken between 25 and 2000  $\mu\text{m}$ , at 100  $\mu\text{m}$  steps (Fig. 1). The data were processed using the Project-FOUR-4.1 (WITec, Ulm, Germany) and Origin (OriginLab Corporation, Northampton, Massachusetts, USA) softwares.

### 3. Results and discussion

#### 3.1. Raman analysis of tumors with and without OCAs

There is still no complete knowledge of the action of skin-clearing agents *in vivo* nor in melanoma. For this reason, it was initially investigated if it was possible to detect OCA-induced modifications through Raman signal, and if so, to track the depth achieved by OCA in the tissue. Figure 2 shows the Raman spectrum of the used clearing agent mixture of PEG-400 and 1,2-propanediol, which is in agreement with the ones reported in the literature [40].

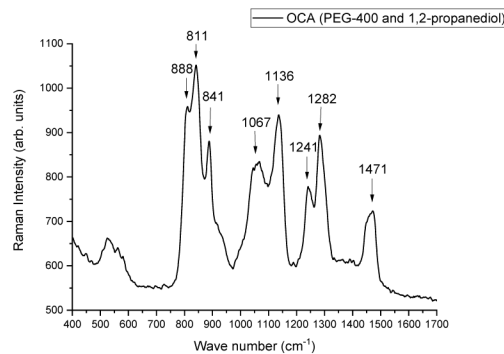


**Fig. 2.** Raman spectrum of optical clearing agents (PEG-400 and 1,2-propanediol).

Raman spectra from melanoma tumor slides with and without OCA treatment were recorded. Three main regions of the tumor were chosen for Raman analysis: 25–125  $\mu\text{m}$  considering the most superficial region of the melanoma; 225–325  $\mu\text{m}$  for the central region of the tumor and 525–725  $\mu\text{m}$  for the deepest and internal region of the tumor. This choice was made in order to verify to what depth the OCA could permeate through the tumor, as well as to what depth the agents would cause biochemical changes to the melanoma.

Examples of the spectra obtained at different depths of the melanoma with and without OCA are presented in Fig. 3. The Raman peaks of OCA are in the same region as the spectrum of the tumor tissue with some peaks overlapping the same wavenumbers. Therefore, it was not possible to directly observe the OCA Raman peaks at the OCA-treated melanoma, neither a clear modification of the melanoma Raman spectrum after the OCA treatment (Fig. 3).

In general, the Raman spectra from tissues show noisy patterns and bands with low signal amplitude, instead of sharp clearly defined. The most characteristic peaks of both the control and the tumor with OCA for the most superficial region (25–125  $\mu\text{m}$ ) are presented in Table 1. In the spectrum of normal skin, the most characteristic peaks referred mainly to actin, collagen, and elastin are 857, 939, 1004, 1248, 1271, and 1452  $\text{cm}^{-1}$  [32]. There are also related peaks in the region of 400 to 1000  $\text{cm}^{-1}$ , but with low amplitudes. The 1270–1300  $\text{cm}^{-1}$  band and the peak 1452  $\text{cm}^{-1}$  can be attributed to the saturated fatty acid of the epidermis ceramides and the cell membrane phospholipids [32]. Other peaks of unsaturated lipids appear as 1092, 1271, 1301, 1452 and 1658  $\text{cm}^{-1}$  [32]. Comparing the spectra of normal skin and melanoma, it is possible to infer

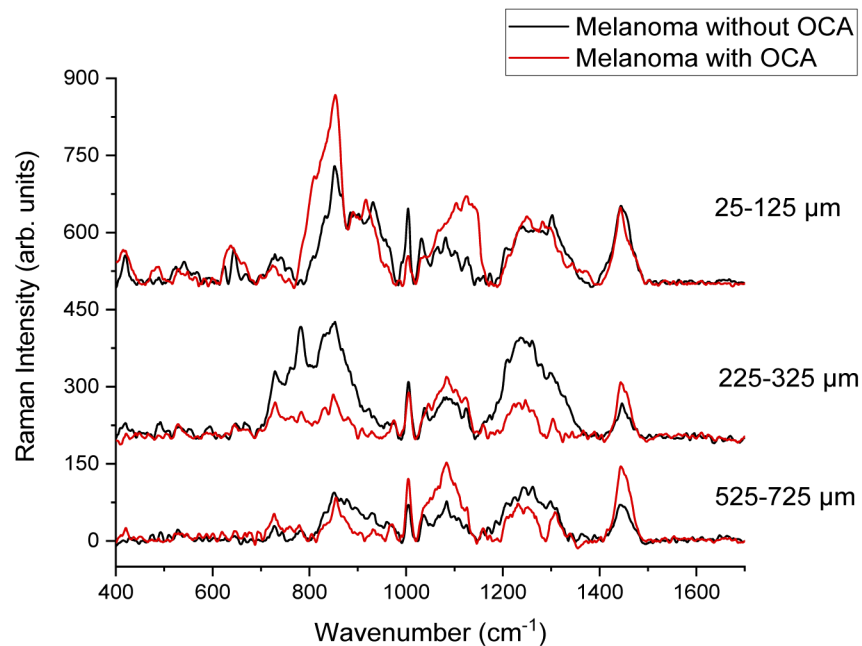


**Fig. 3.** Raman spectra of melanoma at different depths: 25-125  $\mu\text{m}$ , 225-325  $\mu\text{m}$ , and 525-725  $\mu\text{m}$  after OCA application compared to the melanoma without OCA topical application.

that some peaks in the region of 800-1000  $\text{cm}^{-1}$  and 1200-1400  $\text{cm}^{-1}$  are slightly shifted, with different intensities [32,41]. The melanoma peaks are more similar to the normal skin in the most superficial region. Stremersch *et al.* [42] obtained Raman spectra using surface enhanced Raman spectroscopy (SERS) of B16-F10 melanoma cells, with gold nanoparticles. Brauchle *et al.* [43] used Raman Spectroscopy to distinguish different types of melanoma cells from melanocytes. Both in the Stremersch and Brauchle studies, the spectra of melanoma cells showed similar peaks better defined in 780, 980, 1000, 1050, and 1236  $\text{cm}^{-1}$  in the studies with nanoparticles [42,43]. The tumor Raman spectra in our experiments, on the other hand, present the peaks previously mentioned, but with the presence of noise, since no enhancement was used, and because there is a great variety of molecules present in the tumor that contribute to the Raman signal. The resulting signal collected is composed of all biomolecules present in the tissue (cells and extracellular matrix), in addition to the light-tissue interactions being much more complex when compared than those occurring in cells or solutions.

The highest change after OCA addition occurred in the 850-1130  $\text{cm}^{-1}$  region, where the Raman peaks of the C-C backbone of proteins and lipids are located [44], indicating that the vibrations of the protein and lipid skeleton and the conformation of proteins (collagen) are among the most affected by the optical clearing.

In the region of the tumor between 225 and 325  $\mu\text{m}$  (Fig. 2), several Raman peaks also changed their amplitudes in the presence of OCA. No clear distinction was observed when comparing the intensities of the same peaks of tumor with and without OCA. The differences in intensities between the peaks occur in proteins, lipids, and nucleic acids (according to Table 1 references) and may be due to conformational changes in collagen, with the number of alpha-helices being changed and the proportion of beta-sheet and random coil conformations as well [48]. The OCA appears to cause dissociation of collagen fibrils into microfibrils, thus changing the packaging of collagen in the tumor [35,36,49]. Collagen fibers are complex and highly scattering structures,



**Table 1. Raman peaks and their referenced band assignments for 25-125  $\mu\text{m}$ , 225-325  $\mu\text{m}$  and 525-725  $\mu\text{m}$ .**

Raman peaks ( $\text{cm}^{-1}$ )	Band assignments	Depth $\mu\text{m}$		
		25-125	225-325	525-725
488	Glycogen polysaccharide [42,44]	+		
728	C-C bond of collagen proline and the amino acid alanine [43,44]		+	+
780	Breathing modes of the base rings in the DNA / RNA [43,44]		+	
850-854	Single-link stretch vibrations of amino acids, and polysaccharides; tyrosine and the breathing of its ring (proteins); stretch C-C of the proline ring; (C-O-C) skeletal mode of anomers [44]	+	+	+
928	C-C bond of amino acids such as proline and valine [44]			+
1000-1004	Phenylalanine bonds. At 1004 $\text{cm}^{-1}$ is the C-C bond in the ring, mainly collagen [43-46]	+	+	+
1031	Phenylalanine C-H bond; collagen residues; C-N binding of proteins [44]	+	+	
1032	Collagen and phospholipid CH <sub>2</sub> CH <sub>3</sub> bonds [42-44]		+	
1083	C-N binding of proteins and lipids [44]		+	+
1100	C-C bonds of lipids and fatty acids [44]	+		
1124	C-C bonds of lipids and fatty acids [42,44]	+		
1206	Hydroxyproline and tyrosine [44]			+
1224	$\beta$ sheet amide III [44,47]			+
1236	Amide III [47]		+	
1241	Asymmetric phosphate PO <sub>2</sub> originated from the nucleic acid phosphodiester groups in malignant tissues [44,47]			+
1250	Amide III (( $\beta$ -sheet and random coil conformations); guanine and cytosine (NH <sub>2</sub> ) [44,46,47]	+		
1261	Amide III and lipid CH <sub>2</sub> binding [44,47]			+
1296	CH <sub>2</sub> strain [44]		+	+
1298	Deformation and twist of the lipid CH <sub>2</sub> bond [43,44,47]			+
1443	CH <sub>2</sub> deformation of lipids and proteins; triglycerides (fatty acids) and cholesterol [42,44,47]		+	+

and the main bonding force that unites triple helices is hydrogen bonds [35,49]. OCA, which have several hydroxyl groups, destabilize the ordered structure of the fibers, dissociating them, but this can be easily reversible because the interactions are non-covalent bonds between the fibers [35]. Yeh *et al.* observed this fact in an *in vitro* experiment immersing a tissue in glycerol and later in phosphate-buffered saline (PBS) [50]. R. Millon *et al.* also studied the effect of some OCA like PBS and DMSO *in vivo* on a squamous epithelium [34]. Because OCA dehydrate the tissue, there is an increase in the osmolarity of the interstitial fluid, causing the water to escape from the cells and collagen fibers. This results in a decrease of tissue thickness, leading to a denser tissue with more orderly architecture [33,35,36,49]. Sdobnov *et al.* [51] performed a quantitative analysis of the ratio of the collagen Raman peaks intensity after the application of two types of OCA, glycerol, and iohexol (Omnipaque). The authors observed that the intensity of the peaks increased with the application of both agents to the pig skin dermis, which may result from a more compact structure of collagen fibers [51]. Nguyen *et al.* used Raman spectroscopy to verify the behavior of collagen with water, differentiating the age of the skin [52]. It was verified that

there is a variation in the Raman signal, mainly due to the difference in intensity of some peaks related to the hydration marking of the biological sample [52,53]. Therefore, it is expected that the application of OCA in tumors will generate a change in the Raman signal of collagen.

Finally, in the region between 525  $\mu\text{m}$  and 725  $\mu\text{m}$  (Fig. 3), other peaks, that were not previously seen nor identified presented greater intensity. They correspond to proline, tyrosine and valine amino acids, amide III, proteins, lipids, and phosphate from nucleic acids [43–47].

Deeper than 725  $\mu\text{m}$ , the spectra of the tumor with OCA showed little difference between the tumors with and without OCA. Since the difference between spectra is insignificant, this may indicate that the clearing agents did not penetrate above this depth and had little or no effect in the tumor and, consequently, on the light penetration. Yanina *et al.* [54] investigated different concentrations of glycerol solutions as OCA in an *ex vivo* model of pig skin. Maximum penetration, evaluated by confocal Raman microspectroscopy, down to the depth of 80  $\mu\text{m}$  was achieved with a 60% glycerol and 40% water for 45 min of application. Sdobnov and collaborators [55] reported the increased depth Raman spectral changes of the hydrogen bound water, at the *ex vivo* porcine skin, with increased OCA treatment time, both for glycerol and Omnipaque clearing solutions. Our results are in agreement with these reported results on the decrease of light attenuation effect of the OCAs in skin, even though a direct comparison of the at-depth response is not possible, since distinct OCA compositions were used; and *ex vivo* and *in vivo* skin presents different OCA diffusion patterns. Lin *et al.* [56] compared the optical clearing effect of 3 different agents (glycerol, iohexol and polyethylene glycol) and serial concentrations at *in vivo* human skin. They report that the three investigated agents enhanced the optical clearing effect on skin, and that the dehydration mechanism, which occurs at the initial treatment period between 10-20 min, reduces the OC. In our *in vivo* cutaneous melanoma model, we have indirectly observed the enhanced optical clearing through the improved PDT response. This result is in agreement with our previous study where we investigated the use of OCA using optical coherence tomography at the same cutaneous melanoma model. Using the OCA previous to the OCT resulted in improved imaging up to 750  $\mu\text{m}$  [38].

To check if it was possible to determine the maximum penetration depth of OCA in melanoma, a mathematical analysis of the spectra taken from melanoma slides with and without previous OCA treatment was performed. First, normalization was performed at the wavenumber of the highest amplitude of all spectra. Melanoma spectrum obtained from the most superficial region of the tumor (25-125  $\mu\text{m}$ ) was summed to the OCA spectrum. Each final spectrum was then compared with the spectrum taken at melanoma treated with the OCA. It was analyzed which peaks increased their intensities and whether it was possible to verify the presence of OCA by Raman spectroscopy. It was observed that some peaks, such as 850, 1082, and 1240  $\text{cm}^{-1}$  showed higher intensities, probably due to OCA presence. The main region of increased amplitude was over 1003  $\text{cm}^{-1}$ , in which the peaks are more pronounced than in the melanoma without OCA. Even though these changes could be observed at the comparison between the processed spectra and the spectra from melanoma with OCA, they were not evident enough to directly detect the presence of OCA, mainly because melanoma itself already shows Raman peaks at the same region.

### 3.2. Raman analysis of tumors with and without OCAs right after PDT

Representative spectra (Fig. 4) taken at the melanoma lesion at different depths after PDT treatment with and without OCA.

At the more superficial region (25-125  $\mu\text{m}$ ), there was no difference in the spectra of tumors treated with PDT and with and without OCA topical application (Fig. 4). The spectra taken at this depth were similar within the same treatment group and also inter-groups, highly noisy and with a relevant decrease in the Raman signal when compared to the non-treated melanoma. This is probably a result of PDT destruction of the biomolecules and tumor structure in this region.

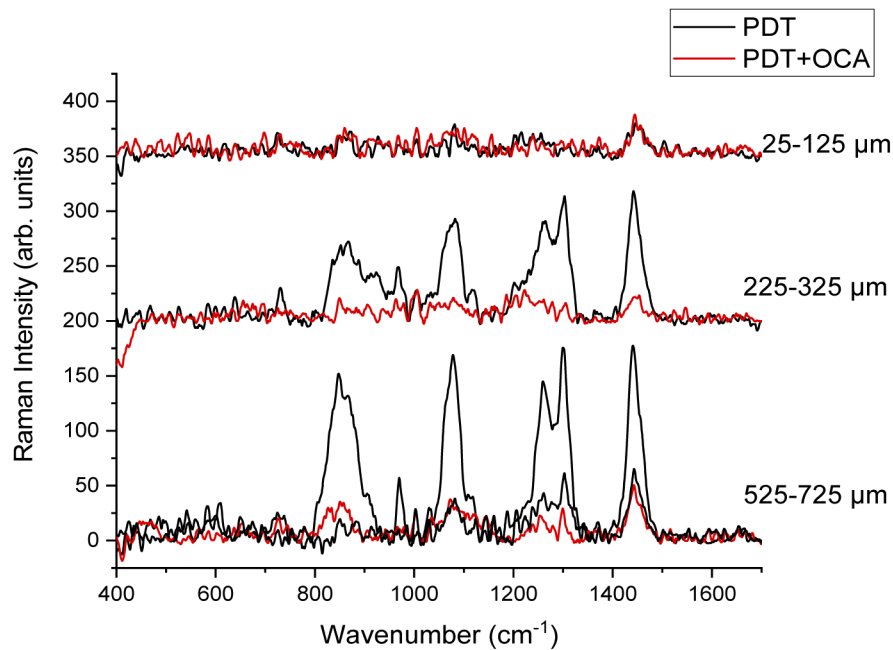


**Fig. 4.** Raman spectra of the 25-125  $\mu\text{m}$ , 225-325  $\mu\text{m}$ , and 525-725  $\mu\text{m}$  regions of PDT-treated melanoma lesions with and without OCA. For the 525-725  $\mu\text{m}$  region, two spectra are presented for the PDT group due to the dual behavior of the observed response: one with a more similar spectrum comparing to the ones collected at the superficial regions, while the other, similar to a non-treated tumor.

Similar results between the groups can be explained by the fact that at the superficial layers of the tumor, no relevant light attenuation is observed, resulting in a homogenous PDT effect within this tumor volume and no changes in the response are observed with the OCA combination.

When evaluating the region between 225  $\mu\text{m}$  and 325  $\mu\text{m}$  (Fig. 4), the spectra from tumors treated only with PDT or PDT + OCA showed mostly changes in the intensity profile, no new Raman peaks nor relevant displacements were present. It is possible to observe that all the peaks showed their intensity decreased when the OCA was applied before PDT. The spectrum from the PDT group without OCA is more similar to the ones measured from non-treated tumors. The PDT + OCA spectrum is similar to the spectra collected at the most superficial part of the tumor. Based on these results, there is an indication that the OCA use has minimized the effect of light attenuation at the melanoma depth of 225-325  $\mu\text{m}$ , resulting in a more effective PDT response similar to the superficial tumor region.

The spectra from the region between 525  $\mu\text{m}$  and 725  $\mu\text{m}$  (Fig. 4) of the PDT group, showed a dual behavior where there were spectra similar to the spectrum of a non-treated tumor and a tumor showing PDT response. On the other hand, the spectra from the PDT + OCA group at this depth were similar to the ones measured at the superficial region, *i.e.* with the PDT response. The variation in the shape of the spectra is due to the tumor heterogeneity, but also the heterogeneity of the photodynamic response at greater depths. Heterogeneous PDT response within the tumor means that non-treated regions with viable melanoma may result in tumor regrowth.

More similar spectra after PDT + OCA treatment at the studied depths down to 750  $\mu\text{m}$  are indicative that a more homogeneous and effective PDT response was achieved. We hypothesize that the OCA, by improving the refractive index matching resulted and making tumors more optically homogeneous, lead to a more effective photodynamic response. This is a relevant



result since the heterogeneity of tumor irradiation is one of the most important reasons that result in treatment failed, since islands of tumor cells remain viable. Based on these results, we hypothesize that OCA would also be beneficial to other pigmented lesions, as pigmented basal cell carcinoma, and also to thicker tumors, the last case, if other delivery methods are developed to increase OCA depth distribution.

### 3.3. Raman analysis of tumors with and without OCAs 7 days after PDT

In order to evaluate if the addition of the OCA to the subdose PDT treatment would result in a modified tumor regrowth, Raman spectra were also recorded at 7 days post-PDT. Figure 5 shows Raman spectra recorded from these regrown melanomas. No relevant changes were observed in the spectra from different depths and treated groups when compared to the non-treated tumors. In this sense, when a partial response is achieved after OCA are used in combination with PDT, which was planned for this study, the resulted regrown tumor did not show biochemical changes evident by Raman spectroscopy. This behavior should be also investigated by other methods such as immunohistochemistry and longer follow up period, but Raman spectroscopy provides a preliminary indicative.

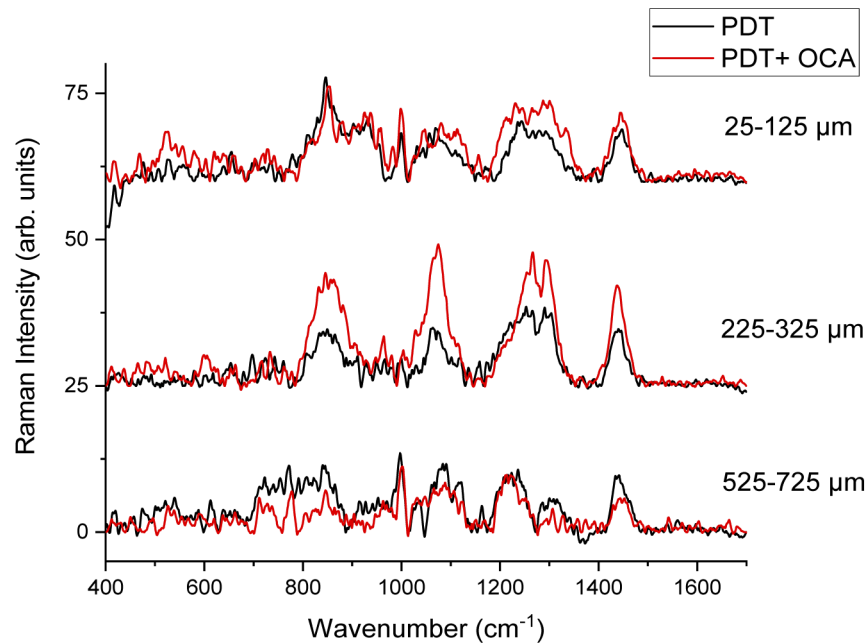


**Fig. 5.** Raman spectra of the 25-125  $\mu\text{m}$ , 225-325  $\mu\text{m}$  and 525-725  $\mu\text{m}$  regions of melanoma with and without OCA 7 days after PDT-treatment.

## 4. Conclusions

PDT shows a limited effect on pigmented lesions, since it highly relies on a homogenous light distribution within the tumor to result in an effective response. Cutaneous melanoma commonly shows heterogenous micro-regional tissue characteristics, and, consequently, heterogeneous optical properties. In the present study, we evaluated the melanoma changes after the treatment of OCA and PDT. The main biochemical changes detected through Raman spectroscopy in the treated tumor were in proteins, lipids and nucleic acids. Due to the refractive index matching, light penetration and distribution was increased in the OCA-treated tumors. OCA topical application

before tumor irradiation resulted in more homogenous, deeper and improved PDT treatment down to 750  $\mu\text{m}$  in cutaneous pigmented melanoma.

## Funding

Conselho Nacional de Desenvolvimento Científico e Tecnológico (131695/2018-5, 305795/2016-3, 465360/2014-9); Fundação de Amparo à Pesquisa do Estado de São Paulo (2013/07276-1, 2014/50857-8).

## Disclosures

The authors declare that there are no conflicts of interest related to this article.

See [Supplement 1](#) for supporting content.

## References

1. A. E. Chang, L. H. Karnell, and H. R. Menck, "The National Cancer Data Base Report on Cutaneous and Noncutaneous Melanoma," *Cancer* **83**(8), 1664–1678 (1998).
2. E. Aladowicz, L. Ferro, G. C. Vitali, E. Venditti, L. Fornasari, and L. Lanfrancione, "Molecular networks in melanoma invasion and metastasis," *Futur. Oncol.* **9**(5), 713–726 (2013).
3. A. M. C. Pinheiro, H. Friedman, A. L. S. V. Cabral, and H. A. Rodrigues, "Melanoma cutâneo: características clínicas, epidemiológicas e histopatológicas no Hospital Universitário de Brasília entre janeiro de 1994 e abril de 1999," *An. Bras. Dermatol.* **78**(2), 179–186 (2003).
4. I. Zalaudek, G. Ferrara, G. Argenziano, V. Ruocco, and H. P. Soyer, "Diagnosis and treatment of cutaneous melanoma: a practical guide," *SKINmed: Dermatology for the Clinician* **2**(1), 20–33 (2003).
5. A. M. M. Eggermont, A. Spatz, and C. Robert, "Cutaneous melanoma," in *The Lancet* (Lancet Publishing Group, 2014), **383**(9919), pp. 816–827.
6. A. Breslow, "Thickness, Cross-Sectional Areas and Depth of Invasion in the Prognosis of Cutaneous Melanoma," *Ann. Surg.* **172**(5), 902–908 (1970).
7. A. Marine and B. Walter, *Non-Invasive Determination of Breslow Index* (Intech, n.d.).
8. M. J. Sladden, O. E. Nieweg, J. Howle, B. J. Coventry, and J. F. Thompson, "Updated evidence-based clinical practice guidelines for the diagnosis and management of melanoma: Definitive excision margins for primary cutaneous melanoma," *Med. J. Aust.* **208**(3), 137–142 (2018).
9. M. Berwick, E. Erdei, and J. Hay, "Melanoma Epidemiology and Public Health," *Dermatol. Clin.* **27**(2), 205–214 (2009).
10. R. J. Sullivan, M. B. Atkins, J. M. Kirkwood, S. S. Agarwala, J. I. Clark, M. S. Ernstoff, L. Fecher, T. F. Gajewski, B. Gastman, D. H. Lawson, J. Lutzky, D. F. McDermott, K. A. Margolin, J. M. Mehnert, A. C. Pavlick, J. M. Richards, K. M. Rubin, W. Sharfman, S. Silverstein, C. L. Slingluff, V. K. Sondak, A. A. Tarhini, J. A. Thompson, W. J. Urba, R. L. White, E. D. Whitman, F. S. Hodi, and H. L. Kaufman, "An update on the Society for Immunotherapy of Cancer consensus statement on tumor immunotherapy for the treatment of cutaneous melanoma: Version 2.0," *J. Immunother. Cancer* **6**(1), 44 (2018).
11. A. M. M. Eggermont, A. Testori, M. Maio, and C. Robert, "AntiCTLA-4 antibody adjuvant therapy in melanoma," *Semin. Oncol.* **37**(5), 455–459 (2010).
12. A. M. Di Giacomo, R. Danielli, M. Guidoboni, L. Calabrò, D. Carlucci, C. Miracco, L. Volterrani, M. A. Mazzei, M. Biagioli, M. Altomonte, and M. Maio, "Therapeutic efficacy of ipilimumab, an anti-CTLA-4 monoclonal antibody, in patients with metastatic melanoma unresponsive to prior systemic treatments: Clinical and immunological evidence from three patient cases," *Cancer Immunol. Immunother.* **58**(8), 1297–1306 (2009).
13. S. B. Brown, E. A. Brown, and I. Walker, "The present and future role of photodynamic therapy in cancer treatment," *Lancet Oncol.* **5**(8), 497–508 (2004).
14. K. Moghissi and K. Dixon, "Photodynamic therapy (PDT) in esophageal cancer: A surgical view of its indications based on 14 years experience," *Technol. Cancer Res. Treat.* **2**(4), 319–326 (2003).
15. P. Agostinis, K. Berg, K. A. Cengel, T. H. Foster, A. W. Girotti, S. O. Gollnick, S. M. Hahn, M. R. Hamblin, A. Juzeniene, D. Kessel, M. Korbelik, J. Moan, P. Mroz, D. Nowis, J. Piette, B. C. Wilson, and J. Golab, "Photodynamic therapy of cancer: An update," *CA. Cancer J. Clin.* **61**(4), 250–281 (2011).
16. Y. Hayata, H. Kato, H. Okitsu, M. Kawaguchi, and C. Konaka, "Photodynamic therapy with hematoporphyrin derivative in cancer of the upper gastrointestinal tract," *Semin. Surg. Oncol.* **1**(1), 1–11 (1985).
17. B. P. Shumaker and F. W. Hetzel, "Clinical laser Photodynamic Therapy in the Treatment of Bladder Carcinoma," *Photochem. Photobiol.* **46**(5), 899–901 (1987).

18. T. J. Dougherty, C. J. Gomer, B. W. Henderson, G. Jori, D. Kessel, M. Korbek, J. Moan, and Q. Peng, "Photodynamic Therapy," *J. Natl. Cancer Inst.* **90**(12), 889–905 (1998).
19. D. W. Felsher, "Cancer revoked: oncogenes as therapeutic targets," *Nat. Rev. Cancer* **3**(5), 375–379 (2003).
20. D. P. Ramirez, C. Kurachi, N. M. Inada, L. T. Moriyama, A. G. Salvio, J. D. Vollet Filho, L. Pires, H. H. Buzzá, C. T. de Andrade, C. Greco, and V. S. Bagnato, "Experience and BCC subtypes as determinants of MAL-PDT response: Preliminary results of a national Brazilian project," *Photodiagn. Photodyn. Ther.* **11**(1), 22–26 (2014).
21. M. A. Calin and S. V. Parasca, "Photodynamic therapy in oncology," in *Journal of Optoelectronics and Advanced Materials* (National Institute of Optoelectronics, 2006), **8**(3), pp. 1173–1179.
22. D. P. Ramirez, L. T. Moriyama, E. R. de Oliveira, N. M. Inada, V. S. Bagnato, C. Kurachi, and A. G. Salvio, "Single visit PDT for basal cell carcinoma – A new therapeutic protocol," *Photodiagn. Photodyn. Ther.* **26**, 375–382 (2019).
23. P. Mroz, Y. Huang, A. Szokalska, T. Zhiyentayev, S. Janjua, A. Nifli, M. E. Sherwood, C. Ruzié, K. E. Borbas, D. Fan, M. Kraye, T. Balasubramanian, E. Yang, H. L. Kee, C. Kirmaier, J. R. Diers, D. F. Bocian, D. Holten, J. S. Lindsey, and M. R. Hamblin, "Stable synthetic bacteriochlorins overcome the resistance of melanoma to photodynamic therapy," *FASEB J.* **24**(9), 3160–3170 (2010).
24. B. Pucelik, L. G. Arnaut, G. Stochel, and J. M. Dabrowski, "Design of Pluronic-Based Formulation for Enhanced Redaporfin-Photodynamic Therapy against Pigmented Melanoma," *ACS Appl. Mater. Interfaces* **8**(34), 22039–22055 (2016).
25. M. Wagner, E. R. Suarez, T. R. Theodoro, C. D. A. S. Machado Filho, M. F. M. Gama, J. P. Tardivo, F. M. Paschoal, and M. A. S. Pinhal, "Methylene blue photodynamic therapy in malignant melanoma decreases expression of proliferating cell nuclear antigen and heparanases," *Clin. Exp. Dermatol.* **37**(5), 527–533 (2012).
26. J. P. Tardivo, A. Del Giglio, L. H. C. Paschoal, A. S. Ito, and M. S. Baptista, "Treatment of melanoma lesions using methylene blue and RL50 light source," *Photodiagn. Photodyn. Ther.* **1**(4), 345–346 (2004).
27. I. Baldea and A. Filip, "Photodynamic Therapy in Melanoma-An Update," *Journal of Physiology and Pharmacology* **63**(2), 109 (2012).
28. Y.-Y. Huang, D. Vecchio, P. Avci, R. Yin, M. Garcia-Diaz, and M. R. Hamblin, "Melanoma resistance to photodynamic therapy: new insights," *Biol. Chem.* **394**(2), 239–250 (2013).
29. Z. Wang, J. Dillon, and E. R. Gaillard, "Antioxidant Properties of Melanin in Retinal Pigment Epithelial Cells," *Photochem. Photobiol.* **82**(2), 474 (2006).
30. C. Ramachandran, Z. Kang Yuan, X. L. Huang, and A. Krishan, "Doxorubicin Resistance in Human Melanoma Cells: MDR-1 and Glutathione S-Transferase n Gene Expression," *Biochem. Pharmacol.* **45**(3), 743–751 (1993).
31. B. S. Kalal, D. Upadhy, and V. R. Pai, "Chemotherapy resistance mechanisms in advanced skin cancer," *Oncol. Rev.* **11**(1), 19–25 (2017).
32. B. Bodanese, F. L. Silveira, R. A. Zângaro, M. T. T. Pacheco, C. A. Pasqualucci, and L. Silveira, "Discrimination of basal cell carcinoma and melanoma from normal skin biopsies in vitro through raman spectroscopy and principal component analysis," *Photomed. Laser Surg.* **30**(7), 381–387 (2012).
33. K. V. Larin, M. G. Ghosn, A. N. Bashkatov, E. A. Genina, N. A. Trunina, and V. V. Tuchin, "Optical Clearing for OCT Image Enhancement and In-Depth Monitoring of Molecular Diffusion," *IEEE J. Sel. Top. Quantum Electron.* **18**(3), 1244–1259 (2012).
34. S. R. Millon, K. M. Roldan-Perez, K. M. Riching, G. M. Palmer, and N. Ramanujam, "Effect of optical clearing agents on the in vivo optical properties of squamous epithelial tissue," *Lasers Surg. Med.* **38**(10), 920–927 (2006).
35. D. Zhu, K. V. Larin, Q. Luo, and V. V. Tuchin, "Recent progress in tissue optical clearing," *Laser Photonics Rev.* **7**(5), 732–757 (2013).
36. E. A. Genina, A. N. Bashkatov, Y. P. Sinichkin, and V. V. Tuchin, "Optical clearing of skin under action of glycerol: Ex vivo and in vivo investigations," *Opt. Spectrosc.* **109**(2), 225–231 (2010).
37. L. Pires, V. Demidov, B. C. Wilson, A. G. Salvio, L. Moriyama, V. S. Bagnato, I. A. Vitkin, and C. Kurachi, "Dual-agent photodynamic therapy with optical clearing eradicates pigmented melanoma in preclinical tumor models," *Cancers* **12**(7), 1956 (2020).
38. L. Pires, V. Demidov, I. A. Vitkin, V. Bagnato, C. Kurachi, and B. C. Wilson, "Optical clearing of melanoma in vivo: characterization by diffuse reflectance spectroscopy and optical coherence tomography," *J. Biomed. Opt.* **21**(8), 081210 (2016).
39. L. Pires, "Optical strategies for diagnosis and treatment of melanoma," Universidade de São Paulo (2018).
40. H. Rachmawati, B. M. Haryadi, K. Anggadiredja, and V. Suendo, "Intraoral Film Containing Insulin-Phospholipid Microemulsion: Formulation and In Vivo Hypoglycemic Activity Study," *AAPS PharmSciTech* **16**(3), 692–703 (2015).
41. M. Gniadecka, P. A. Philipsen, S. Wessel, R. Gniadecki, H. C. Wulf, S. Sigurdsson, O. F. Nielsen, D. H. Christensen, J. Hercogova, K. Rossen, H. K. Thomsen, and L. K. Hansen, "Melanoma Diagnosis by Raman Spectroscopy and Neural Networks: Structure Alterations in Proteins and Lipids in Intact Cancer Tissue," *J. Invest. Dermatol.* **122**(2), 443–449 (2004).
42. S. Stremersch, M. Marro, B. El Pinchasik, P. Baatsen, A. Hendrix, S. C. De Smedt, P. Loza-Alvarez, A. G. Skirtach, K. Raemdonck, and K. Braeckmans, "Identification of individual exosome-like vesicles by surface enhanced raman spectroscopy," *Small* **12**(24), 3292–3301 (2016).
43. E. Brauchle, S. Noor, E. Holtorf, C. Garbe, K. Schenke-Layland, and C. Busch, "Raman spectroscopy as an analytical tool for melanoma research," *Clin. Exp. Dermatol.* **39**(5), 636–645 (2014).

44. Z. Movasaghi, S. Rehman, and I. U. Rehman, "Raman spectroscopy of biological tissues," *Appl. Spectrosc. Rev.* **42**(5), 493–541 (2007).
45. X. Feng, A. J. Moy, H. T. M. Nguyen, J. Zhang, M. C. Fox, K. R. Sebastian, J. S. Reichenberg, M. K. Markey, and J. W. Tunnell, "Raman active components of skin cancer," *Biomed. Opt. Express* **8**(6), 2835 (2017).
46. A. F. de Oliveira, I. D. de A. O. Santos, S. B. Cartaxo, R. A. Bitar, M. M. S. e. S. Enokihara, H. da Silva Martinho, A. A. Martin, and L. M. Ferreira, "Differential diagnosis in primary and metastatic cutaneous melanoma by FT-Raman spectroscopy," *Acta Cir. Bras.* **25**(5), 434–439 (2010).
47. N. Kourkouvelis, I. Balatsoukas, V. Moulia, A. Elka, G. Gaitanis, and I. D. Bassukas, "Advances in the in vivo Raman spectroscopy of malignant skin tumors using portable instrumentation," *Int. J. Mol. Sci.* **16**(12), 14554–14570 (2015).
48. C. Yorucu, K. Lau, S. Mittar, N. H. Green, A. Raza, I. U. Rehman, and S. MacNeil, "Raman spectroscopy detects melanoma and the tissue surrounding melanoma using tissue-engineered melanoma models," *Appl. Spectrosc. Rev.* **51**(4), 263–277 (2016).
49. A. Y. Sdobnov, M. E. Darwin, E. A. Genina, A. N. Bashkatov, J. Lademann, and V. V. Tuchin, "Recent progress in tissue optical clearing for spectroscopic application," *Spectrochim. Acta, Part A* **197**, 216–229 (2018).
50. A. T. Yeh and J. Hirshburg, "Molecular interactions of exogenous chemical agents with collagen—implications for tissue optical clearing," *J. Biomed. Opt.* **11**(1), 014003 (2006).
51. A. Y. Sdobnov, V. V. Tuchin, J. Lademann, and M. E. Darwin, "Confocal Raman microscopy supported by optical clearing treatment of the skin - Influence on collagen hydration," *J. Phys. D: Appl. Phys.* **50**(28), 285401 (2017).
52. T. T. Nguyen, T. Happillon, J. Feru, S. Brassart-Passco, J. F. Angiboust, M. Manfait, and O. Piot, "Raman comparison of skin dermis of different ages: Focus on spectral markers of collagen hydration," *J. Raman Spectrosc.* **44**(9), 1230–1237 (2013).
53. G. W. Lucassen, P. J. Caspers, and G. J. Puppels, "Water content and water profiles in skin measured by FTIR and Raman spectroscopy," in V. V. Tuchin, ed. (2000), pp. 39–45.
54. I. Y. Yanina, J. Schleusener, J. Lademann, V. V. Tuchin, and M. E. Darwin, "The Effectiveness of Glycerol Solutions for Optical Clearing of the Intact Skin as Measured by Confocal Raman Microspectroscopy," *Opt. Spectrosc.* **128**(6), 759–765 (2020).
55. A. Y. Sdobnov, M. E. Darwin, J. Schleusener, J. Lademann, and V. V. Tuchin, "Hydrogen bound water profiles in the skin influenced by optical clearing molecular agents—Quantitative analysis using confocal Raman microscopy," *J. Biophotonics* **12**(5), e201800283 (2019).
56. Q. Lin, E. N. Lazareva, V. I. Kochubey, Y. Duan, and V. V. Tuchin, "Kinetics of optical clearing of human skin studied in vivo using portable Raman spectroscopy," *Laser Phys. Lett.* **17**(10), 105601 (2020).